Part I: Physical Insight Into Carbon-Doping-Induced Delayed Avalanche Action in GaN Buffer in AlGaN/GaN HEMTs

Vipin Joshi, Shree Prakash Tiwari, *Senior Member, IEEE*, and Mayank Shrivastava, *Senior Member, IEEE*

***Abstract*— Physics behind the improvement in breakdown voltage of AlGaN/GaN HEMTs with carbon-doping of GaN buffer is discussed. Modeling of carbon as acceptor traps and self-compensating acceptor/donor traps is discussed with respect to their impact on avalanche breakdown. Impact of carbon behaving as a donor as well as acceptor traps on electric field relaxation and avalanche generation is discussed in detail to establish the true nature of carbon in GaN that delays the avalanche action. This understanding of the behavior of carbon-doping in GaN buffer is then utilized to discuss design parameters related to carbon doped buffer. Design parameters such as undoped channel thickness and relative trap concentration induced by carbon-doping are discussed with respect to the performance metrics of breakdown voltage, leakage current, sheet charge density, and dynamic ON-resistance.**

***Index Terms*— Acceptor traps, AlGaN/GaN HEMTs, breakdown voltage, buffer designing, carbon-doping, donor traps, self-compensating traps.**

I. Introduction

BUFFER resistivity is a key design parameter to maximize the breakdown voltage (V_{BD}) of AlGaN/GaN HEMTs. Being unintentionally n-type doped, doping of iron(Fe)/carbon(C) is commonly employed to control GaN buffer resistivity. Doping of Fe/C is also known to introduce trap sites in GaN buffer [1]–[6]. C-doping in GaN buffer is widely recognized as an effective method to increase the buffer breakdown voltage [7]. C in GaN can replace Ga or N and behave as either donor or acceptor trap site [3], respectively. This has led to an active debate on the type of traps it introduces [1]–[3], [5], [6]. Different works have presented different models. In few works, C in GaN is proposed to behave as deep acceptor [3], [4], while other works have modeled it in a self-compensating configuration in which it can be present as deep acceptor as well as deep [3] or shallow [1], [2], [5], [6] donor. Experimental works by Fariza *et al.* [8] and Rackauskas *et al.* [9] also suggest self-compensation to be present in C-doped GaN and AlGaN, respectively. Reference [1] suggests C to be present as deep acceptor and compensating shallow donor traps in equal concentration. On the other hand, TCAD-based study in [2] suggests that C in self-compensating configuration with equal donor and acceptor trap concentrations cannot result in experimentally observed current collapse behavior. Furthermore, using density function theory-based calculations, it was suggested that the formation energy required for C to replace Ga in the standard growth conditions (n-type GaN with Ga-face) is very high, making it less probable for C to behave as donor trap site [3].

Although the impact of C-doping, modeled as traps, on the dc-RF dispersion of the device has been well explored [2], [5], [6], the mechanism behind delayed avalanche action or V_{BD} improvement with C-doping is not well understood. A TCAD-based computational study of electric field relaxation resulting from C-doping is presented in [5], which assumed trap concentration to be significantly lower than the C-doping values while using a hole short placed between source/drain contacts and C-doped region. However, deeper insights toward electric field relaxation, which can potentially explain V_{BD} improvement, is missing in earlier works. Moreover, the impact of acceptor traps and the presence of both acceptor and donor traps on avalanche effect is yet to be explored. Beside this, correlation between C-doping and associated trap concentrations is missing in previous works. In this paper, the behavior of C-doping as traps in GaN buffer is discussed in relation with its impact on breakdown voltage of the device. Section II explains the computational framework. Section III discusses the modeling of C-doping in different trap configurations and their impact on V_{BD}. Section IV presents a physical insight into the impact of traps on electric field distribution and avalanche breakdown in AlGaN/GaN HEMT devices. Section V presents AlGaN/GaN channel/buffer stack and C-doping codesign guideline for improved V_{BD} while maintaining low-leakage

Manuscript received October 3, 2018; accepted October 28, 2018. Date of publication November 15, 2018; date of current version December 24, 2018. This work at Indian Institute of Science Bangalore was supported by the Department of Science and Technology, Government of India through Technology Systems Development Programme's under Project DST/TSG/AMT/2015/294. The review of this paper was arranged by Editor G. Meneghesso. *(Corresponding author: Vipin Joshi.)*

V. Joshi was with the Department of Electrical Engineering, IIT Jodhpur, Jodhpur 342037, India, and also with the Department of Electronic Systems Engineering, Indian Institute of Science, Bengaluru 560012, India (e-mail: vipinjoshi@iisc.ac.in).

S. P. Tiwari is with the Department of Electrical Engineering, IIT Jodhpur, Jodhpur 342037, India (e-mail: sptiwari@iitj.ac.in).

M. Shrivastava is with the Advanced Nanoelectronic Device and Circuit Research Laboratory, Department of Electronic Systems Engineering, Indian Institute of Science, Bengaluru 560012, India (e-mail: mayank@iisc.ac.in).

Color versions of one or more of the figures in this paper are available online at http://ieeexplore.ieee.org.

Digital Object Identifier 10.1109/TED.2018.2878770

current and ON-resistance. Finally, this paper is concluded in Section VI.

II. Computational Framework

The computations in this paper were done using Synopsys Sentaurus TCAD [10] suite. Impact ionization was taken into account using the Chynoweth law [11]. The electron and hole impact ionization constants were derived according to the earlier reported works on avalanche breakdown in AlGaN/GaN HEMTs [12], [13]. Polarization-induced fixed charges are considered at all the material interfaces to accurately estimate parasitic channels present in the device, as was reported in [14]. Lattice- and carrier-temperature-related calculations along with quantum correction were found to have negligible impact on V_{BD} and, hence, were neglected in this paper. Contacts with the channel were modeled as Schottky interfaces with lower work function of 4.1 eV to take into account TiN alloy formation and N vacancies at the interface between contact and GaN channel. Modeling aspects related to channel transport, mobility, and sheet charge density (n_S) were calibrated with experimental data according to framework described in our earlier work [14].

The device architecture considered for modeling study is depicted in Fig. 1(a). Schottky-gated nonrecessed devices are considered here to isolate any impact of gate geometry, taking into account only buffer-induced effects on the breakdown performance of the device. For the evaluation of V_{BD}, the device with a threshold voltage of -1 V was biased at $V_{GS} = -5$ V to ensure OFF-state operation. The substrate terminal was kept open so as to reproduce experimental conditions of [7]. It is worth mentioning that with substrate electrode connected to ground the vertical leakage was found to be four orders of magnitude lower when compared to lateral S-D leakage current. Thus, neglecting the vertical leakage current by keeping the substrate terminal open does not affect the discussion and conclusion presented in this paper. Fig. 1(b) depicts an excellent match between TCAD extracted breakdown trends and experimental data [7]. The excellent agreement between the computational and experimental data is achieved by calibrating C-doping-induced donor and acceptor trap concentrations. In addition to this, donor-type surface traps were considered at the AlGaN/passivation layer interface with an activation energy of $E_C - 0.68$ eV [15] and a constant concentration of 1.6×10^{13} cm^{-2}. These surface traps are taken to compensate hole density on surface [14] and the concentration value is selected so as to achieve the required n_S and the gate leakage [14].

III. C-Doping Versus Avalanche Breakdown—Nature of Traps?

Device cross section as shown in Fig. 1(a) is used for computations in this paper. Following device parameters are kept constant at specified values until explicitly stated: source to gate distance (L_{SG}) = 1 μm, gate length (L_{Gate}) = 0.7 μm, L_{GD} = 5 μm, L_{FP} = 0.6 μm, $t_{channel}$ = 35 nm, $t_{C\text{-}Doped}$ = 1.5 μm. An unintentional (n-type) doping of 1×10^{15} cm^{-3} is considered in the GaN buffer [14]. A uniform C-doping is considered in the C-doped GaN buffer region.

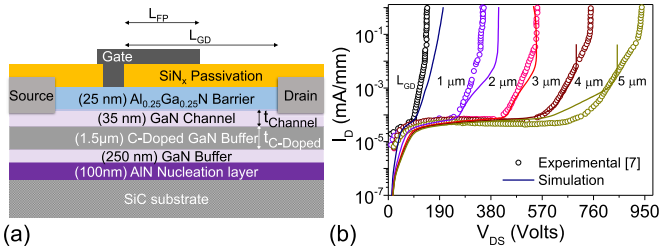

Fig. 1. (a) Carbon-doped AlGaN/GaN HEMT considered in this paper, as adapted from [7]. (b) Comparison of experimental [7] and TCAD computation-based breakdown characteristics of C-doped device with $L_{FP} = 0.6$ μm.

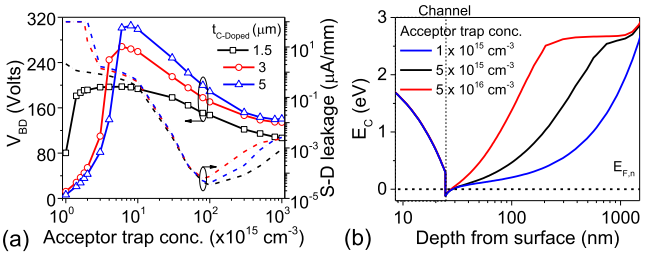

Fig. 2. Impact of acceptor trap concentration, considered in the C-doped region, on (a) V_{BD} and leakage current, extracted at $V_{DS} = 50$ V, in the device, and (b) conduction band energy extracted along a vertical cut-line traversing from AlGaN surface (0 nm) to GaN buffer.

Hence, the trap concentration induced by C-doping will be considered as uniformly distributed in the $t_{C\text{-}Doped}$ thick GaN buffer region. In this section, two possibilities are investigated: 1) C-doping behaving as acceptor traps [2], [3] and 2) C-doping in self-compensating mode where both acceptor and donor traps are considered simultaneously, however with different concentrations and trap energy.

A. Possibility 1: C-Doping as Acceptor Traps

As C is widely debated to behave as acceptor trap in GaN [2], [3], C-doping in this section is modeled as deep acceptor traps with energy $E_V + 0.9$ eV [4]. Impact of the concentration of these acceptor traps on V_{BD} of AlGaN/GaN HEMT device is depicted in Fig. 2(a). It can be observed that V_{BD} initially improves with acceptor trap concentration, saturates to a value at moderate concentrations and then starts decreasing with further increase in acceptor trap concentration. Moreover, V_{BD} was found to increase as the C-doped GaN buffer thickness was increased.

This behavior can be explained as follows. Fig. 2(b) depicts Fermi level to be closer to conduction band for lower acceptor trap concentration in buffer. This leads to buffer leakage-assisted soft breakdown even before avalanche action takes place. In addition to this, electric field peak is located near gate edge for lower acceptor concentration in buffer [Fig. 3(a)] leading to a higher gate leakage in addition to buffer leakage. Increasing acceptor trap concentration in GaN buffer by C-doping shifts Fermi level away from conduction band edge [Fig. 2(b)] and relaxes electric field near the drain side of gate edge [Fig. 3(a)]. This, in turn, controls the buffer leakage and gate leakage, respectively, resulting in an improved V_{BD} [Fig. 2(a)]. The electric field relaxation is attributed to acceptor trap-assisted lateral extension of depletion region.

However, as depicted in Fig. 2(a), V_{BD} falls drastically beyond a certain acceptor trap concentration even when the leakage current continues to fall (or buffer resistivity continues to increase) with increasing acceptor trap concentration. In order to explain this effect, channel (lateral) and buffer (vertical) electric fields for different acceptor trap concentrations are compared in Fig. 3(a) and (b), respectively. Fig. 3(a) indicates that with an increase in acceptor trap concentration as the electric field near the drain side gate edge relaxes, the electric field peak now shifts near the drain edge where the avalanche hot spot is observed. It should be noted that the field is extracted when drain voltage $=V_{BD}$, which is constant initially (at moderate concentrations), however falls at higher trap concentrations. The vertical electric field near the drain edge for a drain bias lower than V_{BD}, as shown in Fig. 3(b), depicts an increase in the peak electric field near drain edge as acceptor trap concentration is increased. As the peak field near the drain edge increases, V_{BD} falls with increase in acceptor trap concentration.

In order to further explain the dependence of the vertical field on acceptor traps [Fig. 3(b)] and field peaking near drain edge, it is important to consider its impact on buffer properties. Apart from affecting the buffer resistivity, acceptor traps in GaN buffer can 1) introduce free holes in GaN buffer, as depicted in Fig. 4(a) and 2) act as charged ions upon ionization, as depicted in Fig. 4(b). In Fig. 4(b), ionized acceptor trap density represents negative charge due to the trapping of an electron. These two factors can change the space charge distribution across the GaN buffer, and hence, can potentially readjust the electric field. It should be noted that a steep increase in hole density can be seen at the end of the GaN buffer (at GaN buffer/AlN nucleation layer interface). This hole density is attributed to polarization charges present at the GaN/AlN interface and is discussed in detail in our earlier work [14]. It is worth mentioning that the compensation of these charges by donor traps with a density of $\sim 4\times 10^{13}$ cm^{-2} had a negligible impact on the distribution of electric field and V_{BD} of the device. As shown in Fig. 4(a), increasing acceptor trap concentration induces free hole density in GaN buffer, which makes it marginally p-type. This results in a reduced buffer resistivity and, hence, reduced V_{BD} due to increased buffer leakage. The trap-induced hole density was found to be orders of magnitude lower than the acceptor trap concentration, which is attributed to the fact that these traps are located deep in the energy gap (0.9 eV away from the valence band edge), and therefore, from Fermi–Dirac statistics can induce a limited number of holes.

In order to understand the later point, i.e., impact of charged ions on vertical field, $t_{Channel}$ as shown in Fig. 1(a) was increased, to shift the ionized charges away from the channel. However, while increasing $t_{Channel}$, $t_{C\text{-}Doped}$ was reduced so as to keep the total buffer thickness unchanged. With this variation, effectively the distance between the positively biased drain electrode and the acceptor trap affected region is increased while maintaining all other parameters constant. This is depicted in Fig. 4(b). Resulting electric field in the channel region, as shown in Fig. 4(c), shows a reduction in electric field near the drain edge as the channel thickness is increased.

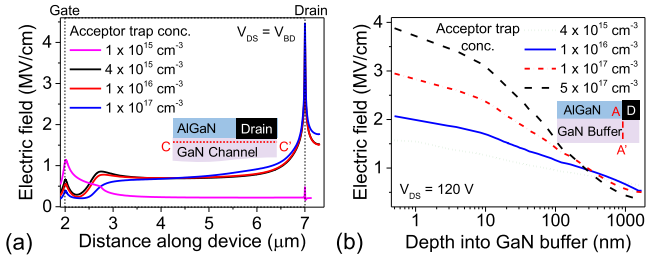

Fig. 3. (a) Lateral electric field extracted at the onset of avalanche breakdown for different acceptor trap concentrations. Avalanche hot spot near the drain edge can be observed in all the cases. (b) Vertical electric field extracted near the drain edge for different acceptor trap concentrations indicating dependence of vertical field on acceptor trap concentration. Inset: cut-line along which electric fields are extracted.

This further quantifies the dependence of electric field on acceptor traps in the buffer region which can now be explained as follows. As acceptor traps ionize by capturing electrons from 2-DEG, they build a negative charge in the buffer region. As these traps are present beneath the drain electrode as well, an electric field exists between the positively biased drain electrode and negatively charged acceptor ions. The peak of this electric field increases as the distance between the drain electrode and trap affected region is reduced [Fig. 4(c)] or if acceptor trap concentration is increased [Fig. 3(b)]. This effect combined with electric field crowding near the drain edge results in reduced V_{BD} of the device at higher acceptor trap concentrations even when the leakage current reduces.

Limited by the parasitic hole density and adverse impact on the vertical electric field, computations suggest V_{BD} to saturate at $\sim$200 V for an $L_{GD}=5$ μm and $t_{C\text{-}Doped}=1.5$ μm, with C-doping modeled as acceptor traps. However, these values are much smaller than the experimentally observed V_{BD} of $\sim$900 V for a C-doping of $\sim 4\times 10^{19}$ cm^{-3} and similar device dimensions [7]. Thus, C behaving only as acceptor traps in GaN buffer cannot completely explain the V_{BD} improvement observed experimentally in earlier works [7].

B. Possibility 2: C-Doping as Self-Compensating Acceptor and Donor Traps

As C behaving as acceptor traps alone is not able to explain experimentally observed improvement in V_{BD}, C-doping is modeled in self-compensating configuration, i.e., as deep acceptor trap with energy $E_V+0.9$ eV [4] and self-compensating donor trap with energy $E_C-0.11$ eV [1], [5], [6]. Fig. 5(a) indicates an improvement in V_{BD} as donor traps are introduced in the C-doped region for a fixed acceptor trap concentration. However, this improvement is limited by acceptor trap concentration present in the C-doped region, with a reduction in V_{BD} observed as donor trap concentration approaches acceptor trap concentration. As can be seen from Fig. 5(b), this reduction in V_{BD} is accompanied by an increased buffer leakage current, suggesting the formation of a parasitic leakage path/channel. Fig. 6(a) depicts a further improvement in V_{BD} with increase in gate to drain spacing (L_{GD}) as the donor trap concentration is increased. This time relatively a higher acceptor trap concentration was used compared to what was used in Fig. 5 to have a higher donor trap concentration without

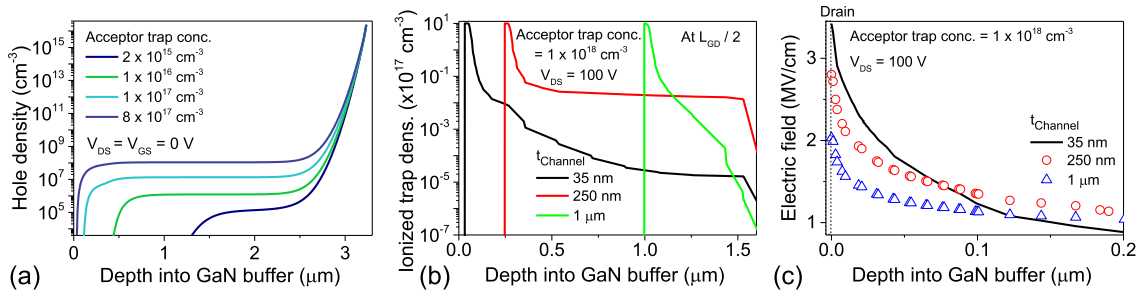

Fig. 4. (a) Impact of C-doping-induced acceptor traps on parasitic hole density in GaN buffer. (b) Ionized acceptor trap profile along a vertical cut line located at a distance of $L_{GD}/2$ from gate edge and extracted for different values of $t_{Channel}$. (c) Vertical electric field, extracted along a vertical cut line near drain edge for different values of $t_{Channel}$, indicating a dependence of electric field peak near drain edge on the channel thickness.

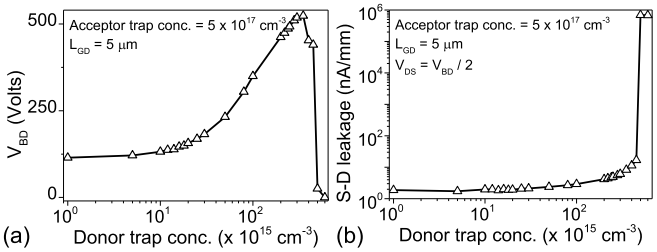

Fig. 5. Impact of donor trap concentration on (a) breakdown voltage of the device and (b) leakage current through the device extracted at $V_{DS} = V_{BD}/2$. Thickness of C-doped region, $t_{C\text{-}Doped} = 1.5\ \mu$m.

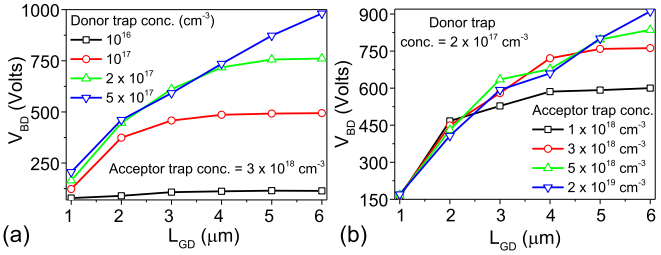

Fig. 6. (a) Impact of donor trap concentration on breakdown voltage as a function of gate to drain spacing (L_{GD}), in presence of acceptor traps induced by C-doping. (b) Impact of increasing acceptor trap concentration in presence of a fixed donor trap concentration on breakdown voltage as a function of L_{GD}. Thickness of C-doped region, $t_{C\text{-}Doped} = 1.5\ \mu$m.

affecting the leakage current. Similar improvement in V_{BD} with L_{GD} is also observed experimentally in earlier works when C-doping concentration was increased [7]. Furthermore, increasing the acceptor trap concentration while having a constant donor trap concentration, as shown in Fig. 6(b), also results in an improved V_{BD}. An agreement with experimental data, as shown in Fig. 1(b), was found for acceptor trap concentration of $\sim 3 \times 10^{18}$ cm^{-3} along with a compensating donor trap concentration of $\sim 5 \times 10^{17}$ cm^{-3}, justifying the use of higher trap concentrations in Fig. 6. From Fig. 6(a) and (b), it can be fairly concluded that the relative concentration of acceptor and donor traps controls the avalanche breakdown in these devices with donor traps having a more pronounced impact on V_{BD}; however, it must stay below the acceptor trap concentration.

IV. Impact of Traps on Avalanche Breakdown—Physical Insight

As discussed in the previous section, the buffer traps are expected to affect the vertical electric field. Hence, the device considered in this section has higher L_{GD} of 10 μm and L_{FP} of 3 μm with a thicker C-doped buffer of 3 μm. This is done to isolate the impact of lateral electric field and to have a better understanding of the impact of traps on the vertical electric field and the avalanche breakdown.

A. Donor Traps: Impact on Free Charge Carriers and Vertical Electric Field in GaN Buffer

The impact of donor traps in the presence of acceptor traps in GaN buffer can be considered to be composed of the following three effects: 1) it can compensate free holes that are introduced by either acceptor traps or e-h pair production due to impact ionization; 2) change in space charge distribution,

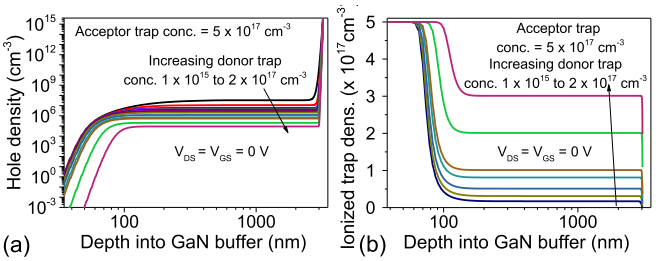

Fig. 7. (a) Reduction in parasitic hole density on compensation by donor traps in the C-doped region. (b) Increase in ionized acceptor trap density in C-doped region on increasing the donor trap concentration.

and therefore, field readjustment due to introduction of free electrons in the buffer; and 3) introduction of ionized traps (fixed charge) in the presence of acceptor traps in the buffer, thereby affecting the vertical electric field due to the change in space charge distribution.

The first aspect that donor traps can compensate free holes is depicted in Fig. 7(a). It can be clearly observed that introducing donor traps can compensate free holes introduced by acceptor traps already present in GaN buffer. The same is expected for holes produced by the onset of impact ionization process, which can potentially delay the impact ionization process. Furthermore, as shown in Fig, 7(b), higher donor trap concentration results in an increased ionized acceptor trap density. Thus, the free electrons induced by donor traps in GaN buffer are trapped in the acceptor traps, and hence, no free electrons are introduced in GaN buffer. This ensures that the introduced donor traps do not contribute in buffer leakage. However, this holds true only if the donor trap concentration is lower than the acceptor trap concentration. As the concentration of donor traps approaches that of acceptor traps, a significant concentration of free electrons will be

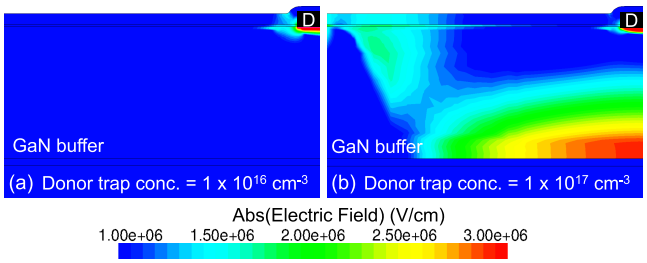

Fig. 8. Electric field contours extracted at the onset of avalanche breakdown with a constant acceptor trap concentration of 5×10^{17} cm^{-3} and a donor trap concentration of (a) 10^{16} cm^{-3} and (b) 10^{17} cm^{-3}. Field redistribution inside GaN buffer can be observed as donor trap concentration is increased.

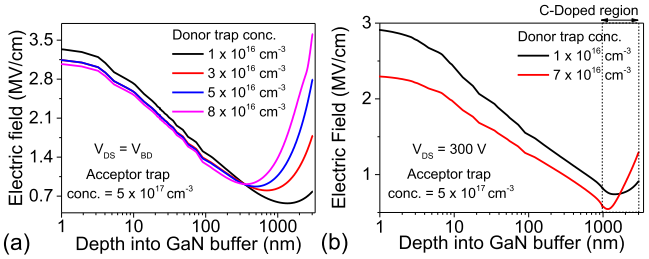

Fig. 9. (a) Redistribution of vertical electric field in the deep GaN buffer observed with increasing donor trap concentration. The electric field is extracted along a cutline through the GaN buffer taken near drain electrode. Channel thickness, t_{Channel}, is taken as 35 nm. (b) Similar redistribution of vertical electric field is observed on increasing t_{Channel} to 1 μm.

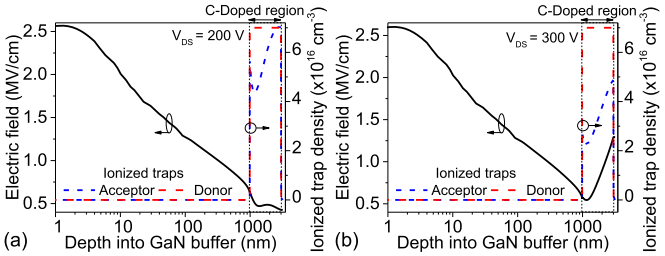

Fig. 10. Vertical electric field along with ionized donor and acceptor trap densities extracted near the drain edge at V_{DS} of (a) 200 V and (b) 300 V. A clear dependence of electric field on ionized trap densities can be observed.

introduced in the GaN buffer, resulting in an increased leakage [Fig. 5(b)]. This also explains the reduction in V_{BD} observed at higher donor trap concentrations in Fig. 5(a).

In order to evaluate the third aspect, i.e., the impact of donor traps on the vertical electric field, electric field contours at the onset of the avalanche breakdown for different donor trap concentrations are compared in Fig. 8. It depicts a higher electric field in the deep GaN buffer region for devices with higher donor trap concentration. Furthermore, the electric field extracted along a cut-line near the drain edge, as shown in Fig. 9(a), indicates an increased redistribution of electric field throughout the GaN buffer as donor trap concentration is increased, which relaxes the electric field peak near the drain edge and increases device's voltage handling capacity. It should be noted that the peak electric field value near the drain electrode remains fixed for all the cases while the absolute drain voltage ($=V_{\text{BD}}$) consistently increases with donor trap concentration. This is attributed to the fact that the electric field profiles are extracted at the onset of the avalanche breakdown, and given that the avalanche hot spot is located at the same point, approximately a fixed peak value (=critical field for impact ionization) is observed. The physics behind the vertical field redistribution with donor traps is explained as follows.

As a significant difference is observed in the electric field in deep GaN buffer region with increase in donor trap concentration, computations were done with increased channel thickness [t_{Channel} in Fig. 1(a)] to investigate the impact of donor traps on electric field. A similar impact on the vertical field can be observed with increase in donor trap concentration even for a channel thickness of 1 μm [Fig. 9(b)]. However, the field redistribution is now limited to the lower buffer region where donor traps were considered. A comparison of the electric field at a drain bias lower than V_{BD}, as shown in Fig. 9(b), clearly depicts that increasing donor trap concentration relaxes the electric field near the drain edge by redistributing it in the buffer region. To evaluate the impact of traps on the electric field distribution, the electric field along with ionized acceptor and donor trap density is compared in Fig. 10. Ionized acceptor and donor traps are compared here as they modify the space charge profile as follows: ionized acceptor traps present negative charge by capturing electron, while donor traps ionize by donating their electron and introduce the positive charge. For lower drain bias voltages, Fig. 10(a) depicts that the positive charge by ionized donor traps is balanced by approximately equal negative charge due to ionized acceptor traps. This results in a nearly constant electric field in this region as $dE/dx \approx qN_{\text{IDT}}/\epsilon_{\text{GaN}} - qN_{\text{IAT}}/\epsilon_{\text{GaN}} \approx 0$, where N_{IDT} = ionized donor trap concentration, N_{IAT} = ionized acceptor trap concentration, and ϵ_{GaN} is the electric permittivity of GaN. On the other hand, Fig. 10(b) depicts that with an increase in drain bias, ionized acceptor trap concentration reduces while ionized donor trap concentration is not affected. This results in a net positive charge in this region due to dominating ionized donor trap concentration. The modified space charge profile enables the vertical electric field to redistribute between the two electric field peaks, one near drain edge and another at the lower edge of donor trap affected region [Fig. 10(b)]. Furthermore, an increase in donor trap concentration increases the net positive charge in this region, leading to an increased field redistribution in the deep GaN buffer [Fig. 9(a)], as $dE/dx \approx q(N_{\text{IDT}} - N_{\text{IAT}})/\epsilon_{\text{GaN}}$. This leads to an improved V_{BD} as donor trap concentration is increased.

Modulation in ionized acceptor and donor trap density under the application of positive drain bias can be explained by considering the trap dynamics. Ionized acceptor traps can detrap by 1) donating their electron and/or 2) capturing a hole. Although detrapping of electron can happen under the applied drain bias, it is less probable as these traps are located deep in the energy band. On the other hand, since these trap levels are located near the valence band, they have a higher tendency to capture holes. These holes are injected by the positively biased drain electrode under the presence of a high electric field near the drain edge. Donor traps being shallow in energy band, are easily ionized by donating electron under the applied

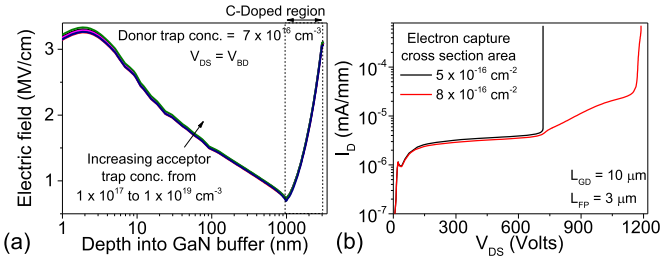

Fig. 11. (a) Impact of increasing acceptor trap concentration on vertical electric field profile near the drain edge. Electric field redistribution in GaN buffer is found to be independent of acceptor trap concentration. (b) OFF-state breakdown characteristics of device with carbon doping modeled as compensating traps and with different electron capture cross-sectional area for acceptor traps. Acceptor trap concentration of 5×10^{17} cm^{-3} and donor trap concentration of 2×10^{17} cm^{-3} were considered.

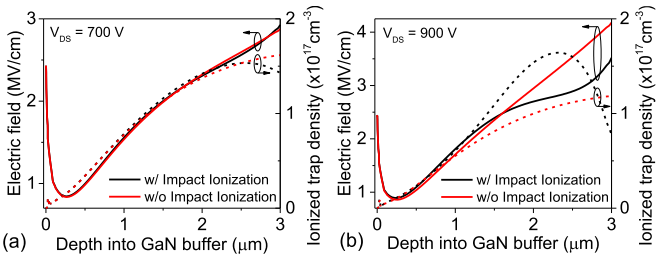

Fig. 12. Electric field and ionized trap density comparison for device when impact ionization was considered and without it, extracted at a drain bias of (a) 700 V and (b) 900 V. Acceptor trap concentration of 5×10^{17} cm^{-3} and donor trap concentration of 2×10^{17} cm^{-3} were considered.

positive drain bias and have less tendency to deionize. This causes a reduction in ionized acceptor trap density as drain bias is increased while the ionized donor trap density remains constant.

B. Acceptor Traps: Impact on Avalanche Generation

A comparison of the vertical electric field near the drain edge at different acceptor trap concentrations for $t_{\text{Channel}} = 1$ μm, as shown in Fig. 11(a), indicates vertical electric field to be independent of acceptor trap concentration. However, Fig. 6(b) suggests an improvement in V_{BD} as acceptor trap concentration is increased, for a reduced t_{Channel} of 35 nm. This suggests acceptor traps to be involved in a mechanism, other than electric field redistribution in the deep GaN buffer region, which assists in V_{BD} improvement. In order to understand the impact of acceptor traps on V_{BD}, electron capture cross section ($A_{\text{eXSection}}$) for these traps was taken as a parameter and device with a reduced t_{Channel} of 35 nm was considered. Fig. 11(b) shows the comparisons of breakdown characteristics of device for two different $A_{\text{eXSection}}$ values. A reduction in V_{BD} from ~1190 to 700 V can be observed with a reduction in $A_{\text{eXSection}}$ from 8×10^{-16} cm^{-2} to 5×10^{-16} cm^{-2}. Furthermore, the I–V characteristics interestingly indicate an increase in current at approximately similar voltage (≈700 V) for both the cases. However, for computations with higher $A_{\text{eXSection}}$, this increase in drain current was suppressed until reaching a hard breakdown at higher V_{DS} values of ~1190 V. This suggests capturing of electrons in acceptor traps to assist in suppressing avalanche generation phenomena, thereby increasing V_{BD}. To have a further insight into this effect, computations were done with $A_{\text{eXSection}}$ of 8×10^{-16} cm^{-2} and the impact of avalanche generation was evaluated by comparing computations with and without accounting for impact ionization.

A comparison of electric field and ionized acceptor trap density at $V_{\text{DS}} = 700$ V for the two cases, as shown in Fig. 12(a), indicates a similar profile. This is also expected as the electric field at this bias voltage is lower than the critical field value, and hence, the avalanche generation is minimum. However, as the drain bias is increased to $V_{\text{DS}} = 900$ V, as shown in Fig. 12(b), a significant difference in the electric field can be observed for the two cases as the electric field in deep GaN buffer crosses the critical field value of ~3 MV/cm. Furthermore, Fig. 12(b) depicts a significant increase in ionized trap concentration when the impact ionization was considered. This can be explained as follows. Electrons generated during the impact ionization in the deep GaN buffer region drift under the influence of drain electric field and is subsequently captured by acceptor traps present in the GaN buffer. This capturing of electrons slows down the avalanche process. In addition to this, capturing of electrons ionizes the acceptor traps and modifies the space charge profile. This is reflected in the electric field as well, as shown in Fig. 12(b), which shows a reduced field in the deep GaN region, thereby further suppressing the avalanche generation. This results in an improvement in V_{BD} as acceptor trap concentration is increased.

It should be noted that practically the trap profile will be different from that considered in these sections and will depend on the activation energies associated with carbon forming acceptor/donor trap sites. However, similar physics will be applicable in those scenarios as well.

C. Combined Impact of Acceptor and Donor Traps

Acceptor traps control avalanche generation by capturing electrons and are responsible for associated field shaping. A similar effect is expected for avalanche generated holes and donor traps. However, donor traps being shallow in nature were found to be completely ionized by either acceptor traps or movement of electrons under drain electric field, thereby limiting the sites available for capturing holes. Thus, donor traps primarily contribute in the electric field redistribution and no such variation with hole capture cross section was observed. Furthermore, as discussed earlier, the peak donor trap concentration that can result in V_{BD} improvement is limited by acceptor traps present in the buffer.

With these observations, it can be fairly concluded that while acceptor traps introduced by C-doping mitigate gate and buffer leakage current, the presence of C in self-compensating configuration with dominating acceptor traps is responsible for the vertical electric field relaxation leading to V_{BD} improvement in AlGaN/GaN HEMT devices.

V. Design Parameters for C-Doped GaN Buffer

A. Channel Thickness

Fig. 13(a) depicts the impact of t_{Channel} on V_{BD} of the device. In these computations, total buffer thickness is kept constant. Thus, with an increase/decrease in the t_{Channel},

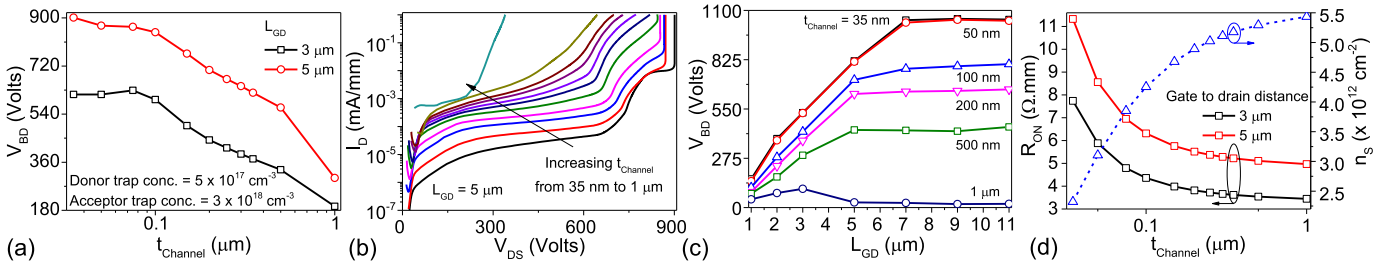

Fig. 13. Impact of undoped channel thickness on (a) breakdown voltage, (b) OFF-state I–V characteristics, (c) improvement in breakdown voltage with lateral scaling of the device, and (d) n_S and ON-resistance of the device. Total buffer thickness is kept constant at 1.785 μm and acceptor and donor trap concentrations are taken as 3×10^{18} cm^{-3} and 5×10^{17} cm^{-3}, respectively. R_{on} was extracted by calculating output characteristics of the device at a gate bias of $V_{GS} = 2$ V. Drain current values were extracted for $V_{DS} = 0.1$ and 0.2 V (both points lie in the linear region of operation). R_{on} was then extracted as $R_{on} = \Delta V/\Delta I = 0.1/\Delta I$, ΔI being the difference in current measured at $V_{DS} = 0.2$ and 0.1 V.

the thickness of the C-doped region is adjusted in order to keep the total buffer thickness constant at 1.785 μm. For leaky devices, the drain voltage at which drain current exceeded the value of 1 mA/mm was considered as V_{BD}. It can be observed from Fig. 13(b) that with increasing $t_{Channel}$, leakage through the device increases. However, it does not significantly affect the hard breakdown or onset of the avalanche effect. This further quantifies the observation that C-doping is responsible for E-field redistribution in the deep GaN buffer regions besides controlling buffer resistivity. This leads to a negligible impact on V_{BD} upto certain channel thickness [Fig. 13(a)]. However, shifting the C-doped region deeper into the GaN buffer increases the gate leakage as well as leakage through the GaN channel which results in significant lowering of V_{BD}. At sufficiently thicker GaN channel ($\sim$1 μm), the breakdown path was formed in the GaN channel with hard breakdown taking place at significantly lower values of drain voltage [Fig. 13(b)]. Furthermore, Fig. 13(c) depicts the impact of $t_{Channel}$ on improvement of V_{BD} with lateral scaling of the device. For channel thickness up to 50 nm, a linear increase in V_{BD} is observed up to L_{GD} of $\sim$7 μm. However, as the channel thickness is increased to 500 nm, V_{BD} starts saturating at a lower L_{GD} of $\sim$5 μm, which can be attributed to increased buffer/gate leakage. As the channel thickness is increased further ($\sim$1 μm), the device breakdown is caused by the leakage current flowing through buffer resulting in a negligible V_{BD} improvement with device lateral scaling. Fig.13(d) suggests a significant improvement in n_S and ON-resistance (R_{ON}) of the device as channel thickness is increased, which is attributed to shift of acceptor traps away from the channel and associated reduction in electron capture by these traps. Interestingly, this improvement is restricted upto a certain thickness ($\sim$250 nm) beyond which it saturates. Based on these guidelines, the channel can be designed to result in an optimized dc performance while maintaining V_{BD} for a given L_{GD}.

B. C-Doping: Optimizing Relative Trap Concentration

From the above-mentioned discussions, it is clear that the presence of acceptor and donor traps in the GaN buffer affects V_{BD}. Moreover, the upper limit on donor trap concentration is decided by the acceptor trap concentration and leakage through the GaN buffer. This section presents the impact of relative

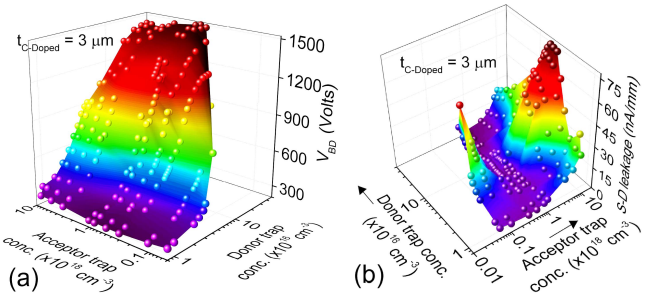

Fig. 14. Impact of relative acceptor and donor trap concentrations induced by C-doping in GaN buffer on (a) breakdown voltage and (b) S-D leakage of the device for a C-doped region thickness of 3 μm. A channel thickness of 35 nm was used. S-D leakage was extracted at $V_{DS} = V_{BD}/2$.

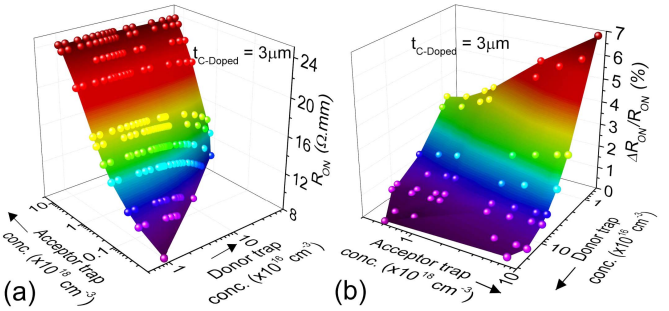

Fig. 15. Impact of C-doping-induced trap concentration on (a) dc ON-resistance and (b) dynamic ON-resistance of the device. Channel thickness was kept constant at 35 nm. Method of extracting the dynamic ON-resistance ($R_{Dynamic}$) of the device and timing specifications of gate and drain pulses were adopted from experimental work in [16]. The quiescent bias conditions were taken as $V_{GS} = -5$ V and $V_{DS} = 45$ V.

donor/acceptor trap concentrations on different device figure of merit parameters, namely, V_{BD}, leakage current, sheet charge density, and ON-resistance. The lateral device dimensions are kept constant at $L_{GD} = 10$ μm, and $L_{FP} = 3$ μm to isolate the effect of lateral electric fields. Furthermore, the channel thickness is kept constant at 35 nm. From Fig. 14(a), it can be observed that irrespective of the acceptor trap concentration, V_{BD} improves with donor trap concentration. Furthermore, improvement with acceptor trap concentration ceases at much lower values. This further emphasizes the importance of relative concentration of acceptor and donor traps induced by C-doping. The leakage current depicted in Fig. 14(b) highlights a window of acceptor trap concentration where the leakage is minimum for a complete range of

donor trap concentration. Thus, with a moderate acceptor trap concentration, donor trap concentration can be maximized to achieve optimum V_{BD} with low-leakage current. Furthermore, the device ON-resistance, as shown in Fig. 15(a) shows dependence on acceptor trap concentration and a weaker dependence on donor trap concentration. This is attributed to the fact that the acceptor traps can capture channel electrons, and hence reduce n_S, whereas donor traps do not affect the channel electron density. Dynamic performance of the device was evaluated by comparing the percentage change in ON-resistance of the device, $\Delta R_{ON}/R_{ON} = (R_{Dynamic} - R_{dc})/R_{dc} \times 100\%$, as a function of C-doping-induced traps in the GaN buffer, shown in Fig. 15(b). It depicts that increasing acceptor trap concentration in the GaN buffer has a negative impact on the dynamic performance of the device as $\Delta R_{ON}/R_{ON}$ increases. However, unlike dc resistance, it is interesting to observe that increasing the donor trap concentration results in a reduction in $\Delta R_{ON}/R_{ON}$, improving the dynamic performance of the device.

A comparative analysis of these parameters suggests a moderate acceptor trap concentration ($\sim 10^{18}$ cm^{-3}) with optimized donor trap concentration ($\sim 5 \times 10^{17}$ cm^{-3}) to maximize V_{BD} while minimizing the leakage, ON-resistance, and dynamic R_{ON}. The behavior of C as donor or acceptor depends on process conditions [3], and hence, an optimization of process conditions can result in the required profile. In addition to this, an experimental method to achieve independent control on acceptor and donor traps in GaN buffer is proposed in part-II of this paper [17]. It should be noted that these trap concentrations are taken without considering any dislocations/defects-induced traps introduced during the epitaxial growth.

VI. Conclusion

Carbon doping modeled as only acceptor traps was found to have a limited impact on V_{BD} of the device. Self-compensating nature of traps introduced by C-doping in GaN was found to be the key parameter controlling V_{BD} in these devices. We established that the donor traps induced by C-doping are important in deciding V_{BD} of the device. However, its concentration is required to be lower than that of acceptor traps in order for the buffer to remain resistive, thereby highlighting the importance of self-compensating nature of traps induced by C in GaN buffer. Space charge modulation by donor traps was found to be the primary reason behind the vertical electric field redistribution improving V_{BD}. On the other hand, acceptor traps introduced by C-doping were found to capture the electrons generated by avalanche phenomena, thereby delaying the avalanche breakdown as well as shaping the electric field in deep GaN buffer. An analysis of design parameters related to buffer designing with C-doping modeled as self-compensating traps suggests an optimum channel thickness which results in a lower ON-resistance while maintaining V_{BD}. Furthermore, TCAD computations suggest a moderate acceptor trap concentration combined with an optimized donor trap concentration to be primary design parameter for optimizing V_{BD}, leakage current, ON-resistance, and dynamic performance of the device.

References

[1] G. Verzellesi *et al.*, "Influence of buffer carbon doping on pulse and AC behavior of insulated-gate field-plated power AlGaN/GaN HEMTs," *IEEE Electron Device Lett.*, vol. 35, no. 4, pp. 443–445, Apr. 2014.

[2] A. Chini *et al.*, "Experimental and numerical analysis of hole emission process from carbon-related traps in GaN buffer layers," *IEEE Trans. Electron Devices*, vol. 63, no. 9, pp. 3473–3478, Sep. 2016.

[3] J. L. Lyons, A. Janotti, and C. G. Van de Walle, "Effects of carbon on the electrical and optical properties of InN, GaN, and AlN," *Phys. Rev. B, Condens. Matter*, vol. 89, no. 3, pp. 035204-1–035204-8, Jan. 2014.

[4] J. L. Lyons, A. Janotti, and C. G. Van de Walle, "Carbon impurities and the yellow luminescence in GaN," *Appl. Phys. Lett.*, vol. 97, no. 10, pp. 152108-1–152108-3, Oct. 2010. DOI: 10.1063/1.3492841

[5] M. J. Uren, M. Caesar, S. Karboyan, P. Moens, P. Vanmeerbeek, and M. Kuball, "Electric field reduction in C-doped AlGaN/GaN on Si high electron mobility transistors," *IEEE Electron Device Lett.*, vol. 36, no. 8, pp. 826–828, Aug. 2015.

[6] M. J. Uren, J. Möreke, and M. Kuball, "Buffer design to minimize current collapse in GaN/AlGaN HFETs," *IEEE Trans. Electron Devices*, vol. 59, no. 12, pp. 3327–3333, Dec. 2012.

[7] E. Bahat-Treidel, F. Brunner, O. Hilt, E. Cho, J. Wurfl, and G. Trankle, "AlGaN/GaN/GaN:C back-barrier HFETs with breakdown voltage of over 1 kV and low $R_{ON} \times$ A," *IEEE Trans. Electron Devices*, vol. 57, no. 11, pp. 3050–3058, Nov. 2010.

[8] A. Fariza *et al.*, "On reduction of current leakage in GaN by carbon-doping," *Appl. Phys. Lett.*, vol. 109, no. 21, p. 212102, 2016. [Online]. Available: https://doi.org/10.1063/1.4968823

[9] B. Rackauskas, M. J. Uren, S. Stoffels, M. Zhao, S. Decoutere, and M. Kuball, "Determination of the self-compensation ratio of carbon in AlGaN for HEMTs," *IEEE Trans. Electron Devices*, vol. 65, no. 5, pp. 1838–1842, May 2018.

[10] *User Manual, Version J-2014.09*, Synopsys TCAD Sentaurus, Synopsys, San Jose, CA, USA, 2014.

[11] A. Chynoweth, "Ionization rates for electrons and holes in silicon," *Phys. Rev.*, vol. 109, no. 5, p. 1537, 1958.

[12] D. Cornigli *et al.*, "Numerical investigation of the lateral and vertical leakage currents and breakdown regimes in GaN-on-Silicon vertical structures," in *IEDM Tech. Dig.*, Dec. 2015, pp. 5.3.1–5.3.4.

[13] F. Monti *et al.*, "Numerical study of GaN-on-Si HEMT breakdown instability accounting for substrate and packaging interactions," in *Proc. IEEE 27th Int. Symp. Power Semiconductor Devices IC's (ISPSD)*, May 2015, pp. 381–384.

[14] V. Joshi, A. Soni, S. P. Tiwari, and M. Shrivastava, "A comprehensive computational modeling approach for AlGaN/GaN HEMTs," *IEEE Trans. Nanotechnol.*, vol. 15, no. 6, pp. 947–955, Nov. 2016.

[15] D. Bisi *et al.*, "Deep-level characterization in GaN HEMTs—Part I: Advantages and limitations of drain current transient measurements," *IEEE Trans. Electron Devices*, vol. 60, no. 10, pp. 3166–3175, Oct. 2013.

[16] Z. Tang, S. Huang, X. Tang, B. Li, and K. J. Chen, "Influence of AlN passivation on dynamic on-resistance and electric field distribution in high-voltage AlGaN/GaN-on-Si HEMTs," *IEEE Trans. Electron Devices*, vol. 61, no. 8, pp. 2785–2792, Aug. 2014.

[17] V. Joshi, S. P. Tiwari, and M. Shrivastava, "Part II: Proposals to independently engineer donor and acceptor trap concentrations in GaN buffer for ultra high breakdown AlGaN/GaN HEMTs," *IEEE Trans. Electron Devices*, vol. 66, no. 1, pp. 570–577, Jan. 2019.

Vipin Joshi has submitted his PhD Thesis in electrical engineering at IIT Jodhpur, Jodhpur, India.

He is currently a Project Scientist with the Indian Institute of Science, Bengaluru, India. His current research interests include modeling and simulation of III-V heterostructures, gate dielectric modeling, and trap characterization in GaN HEMTs and device-circuit co-design.

Shree Prakash Tiwari (M'11–SM'16) received the Ph.D. degree in electrical engineering from IIT Bombay, Mumbai, India, in 2008.

From 2008 to 2011, he was a Post-Doctoral Fellow with the School of ECE, Georgia Institute of Technology, Atlanta, GA, USA. He joined IIT Jodhpur, Jodhpur, India, as an Assistant Professor of electrical engineering in 2011. His current research includes exploration for high performance transistor devices for inorganic and organic/flexible electronics.

Mayank Shrivastava (S'09–M'10–SM'16) received the Ph.D. degree from IIT Bombay, Mumbai, India, in 2010.

He is currently an Assistant Professor with the Department of Electronic Systems Engineering, Indian Institute of Science, Bengaluru, India. He joined the Indian Institute of Science as an Assistant Professor in 2013, where he has established the Advanced Nano Electronic Device and Circuit Research Group.